Model Predictive Control with Delay Compensation for Air-to-Fuel Ratio Control

Sergio Trimboli, Stefano Di Cairano, Alberto Bemporad, and Ilya V. Kolmanovsky

Abstract. To meet increasingly stringent emission regulations modern internal combustion engines require highly accurate control of the air-to-fuel ratio. The performance of the conventional air-to-fuel ratio feedback loop is limited by the combustion delay between fuel injection and engine exhaust, and by the transport delay for the exhaust gas to propagate to the air-to-fuel ratio sensor location. The combined delay is variable, since it depends on engine speed and airflow. Drivability, fuel economy and emission requirements result in constraints on the deviations of the air-to-fuel ratio, stored oxygen in the three-way catalyst, and fuel injection. This paper proposes an approach for air-to-fuel ratio control based on Model Predictive Control (MPC). The approach systematically handles both variable time delays and pointwise-in-time constraints. A delay-free model is considered first, which takes into account the dynamic relations between the injected fuel and the air-to-fuel ratio and the dynamics of the oxygen stored in the catalyst. For the delay-free model, the explicit MPC law is computed. Delay compensation is obtained by estimating the delay online from engine operating conditions, and feeding the MPC law with the state predicted ahead over the time interval of the estimated delay. The predicted state is computed by combining measurement filtering with forward iterations of the nonlinear dynamic equations of the model. The achieved performance in tracking the air-to-fuel ratio and the oxygen storage setpoints while enforcing the constraints is demonstrated in simulation using real data profiles.

Sergio Trimboli · Alberto Bemporad
Department of Mechanical and Structural Engineering, University of Trento, Italy
e-mail: trimboli@ieee.org, bemporad@ing.unitn.it

Stefano Di Cairano
Powertrain Control R&A, Ford Motor Co., Dearborn, MI, US
e-mail: dicairano@ieee.org

Ilya V. Kolmanovsky
Department of Aerospace Engineering, University of Michigan, Ann Arbor, MI, US
e-mail: ilya@umich.edu

R. Sipahi et al. (Eds.): Time Delay Sys.: Methods, Appli. and New Trends, LNCIS 423, pp. 319–330.
springerlink.com

1 Introduction

During recent years tightened emission regulations have been imposed to reduce pollution. In order to meet these regulations without degrading fuel efficiency and vehicle performance, and without embedding excessively expensive hardware components, engineers increasingly rely on improvements in software and controls.

High performance Air-to-Fuel Ratio (AFR) control is critical for emission reductions in spark ignited (SI) engines [5]. The AFR has to be maintained within tight bounds not to degrade vehicle driveability and fuel economy, and to ensure proper functioning of the exhaust aftertreatment system.

The combustion that takes place in the cylinders involves a mixture of air and fuel. For the combustion to be complete, the mass of air and fuel in the mixture must be in a precise ratio, referred to as the *stoichiometric AFR*. The mixture with excess fuel is referred to as *rich*, while the mixture with excess air is referred to as *lean*.

The exhaust gas chemical composition depends on the AFR. The pollutants are converted in the exhaust aftertreatment system, which typically consists of one or more three-way-catalysts (TWC). The TWC converts nitrogen-oxides (NOx), hydrocarbons (HC) and carbon-monoxide (CO) emissions to carbon dioxide and water. In order to maintain high catalyst conversion efficiency, the feedgas AFR must be carefully controlled [5].

The AFR is not directly measured in the cylinder, where the combustion takes place. The feedgas (exhaust gas) AFR is measured by the universal exhaust gas oxygen (UEGO) sensor that is placed close to the TWC inlet, see Fig. 1 where the plant and the control architecture introduced below are shown. Hence, the AFR in the cylinder is controlled by regulating the AFR as measured in the exhaust gas, after the combustion took place and the gas has travelled through the manifold up to the UEGO sensor location.

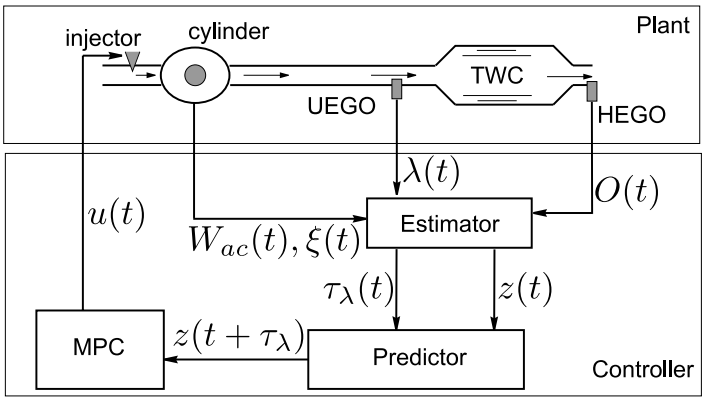

Fig. 1 Schematics of the gas propagation path and AFR-TWC controller architecture.

The dynamics of the air-to-fuel ratio can be represented by a first-order time-delayed system that models the combustion process and the gas transport delay. The transport delay varies up to a factor of 10 depending on the engine operating conditions, as a consequence of the variable exhaust gas pressure and velocity. Since the AFR is affected by disturbances, estimation and actuation errors, and model imprecisions, feedback control is needed. Also, the limits on the injector flow impose constraints on the injected fuel, limiting the actuation range.

Several approaches for controlling AFR have been considered in the literature, see for instance [1, 6, 9] and the references therein. In all of these approaches, AFR has to be regulated to track a time-varying set-point reference. The modulation of the AFR reference may be used to maintain the oxygen storage in the TWC at a desired level and improve catalyst conversion efficiency. A rich mixture causes excess generation of CO and HC in the feedgas, that are converted by the TWC while consuming stored oxygen. A lean mixture may cause an excess of NOx in the feedgas. This NOx is reduced in the TWC and the excess oxygen is stored. If the oxygen storage in the TWC is completely full or completely empty, the TWC cannot efficiently convert the pollutants resulting in emission breakthrough into the tailpipe. Hence, the purpose of controlling the AFR to a given reference is to control the oxygen storage at its desired level, to avoid saturation and depletion. The control of AFR and TWC oxygen is usually solved by an inner-outer loop strategy [6], where the outer-loop controller generates the AFR reference to maintain the oxygen storage at a desired value and the inner-loop controller regulates the AFR to track such a reference, while maintaining it within a range where the vehicle driveability and fuel economy are not degraded. Different design have been proposed for the outer controller, see for instance [4, 7] and the references therein.

In this paper we propose a model predictive control (MPC) approach for controlling the single-input multiple-output (SIMO) system that represents the AFR and oxygen storage dynamics. Even though the system is underactuated, tracking the two setpoints is possible thanks to the integral dynamics of oxygen storage. The MPC can regulate AFR and oxygen storage to track independent references by negotiating the overall system behavior depending on a predefined performance criterion. Furthermore, MPC can explicitly enforce actuation limits and desired operating ranges. Finally, by using explicit model predictive control techniques, the MPC feedback law can be computed in the form of a piecewise affine function [2], which can be evaluated without the need of executing optimization algorithms online, and hence it is suitable for execution on conventional automotive Electronic Control Units (ECU). Due to the time-varying nature of the system and to the presence of time delays, a control architecture is proposed, where a predictor is used to compensate the delays, so that the MPC design can be based on a delay-free model where the state and input bounds are time-varying. As a result of the proposed modelling approach, the explicit MPC law is a function of the current states, references, and time-varying bounds.

The paper is organized as follows. In Sect. 2 the MPC-oriented models of the AFR and of the oxygen storage dynamics are formulated. The delay compensator

and the MPC controller are designed in Sect. 3 and the closed-loop system behavior is simulated in Sect. 4. Conclusions are summarized in Sect. 5.

2 Model of AFR and Oxygen Storage

In this section we discuss the model of the air-to-fuel ratio and of the oxygen storage that will be used for prediction in the model predictive control strategy.

2.1 Air-to-Fuel Ratio Dynamics

The (normalized) Air-to-Fuel Ratio (AFR) λ is defined by

$$\lambda = \frac{1}{\sigma_0}\frac{W_{ac}}{W_{fc}}\,, \tag{1}$$

where W_{ac} [kg/s] is the cylinder air mass flow, W_{fc} [kg/s] is the cylinder base fuel mass flow, and σ_0 is the stoichiometric air-to-fuel ratio, where for the gasoline engines considered in this paper $\sigma_0 = 14.64$. When $\lambda = 1$ the mixture is *stoichiometric*, hence all the air and fuel present in the cylinder are burned. When $\lambda < 1$ the mixture is *rich*, when $\lambda > 1$ the mixture is *lean*.

In AFR control, the objective is for λ to track a reference setpoint by commanding the fuel injectors. The AFR is not measured in the cylinder but after the combustion took place and the exhaust gas has reached the UEGO sensor location. Due to UEGO sensor time-constant, exhaust mixing and cylinder-by-cylinder firing, the AFR dynamics are modelled as a first-order system with delayed input, formulated in discrete time as

$$\lambda(k+1) = \alpha\lambda(k) + \beta u(k - \tau_\lambda(k))\,, \tag{2}$$

where α, β are such that the dc-gain of (2) is 1 (i.e., $\beta = 1-\alpha$), $\tau_\lambda(k)$ is the input time delay, and we consider a sampling period $T_s = 25$ms. The time delay $\tau_\lambda(k)$ in (2) varies depending on the engine operating conditions [6], the airflow W_{ac} and the engine speed ξ [rpm]

$$\tau_\lambda(k) = \alpha_0 + \frac{\alpha_1}{\xi(kT_s)} + \frac{\alpha_2 M_{\max}(\xi(kT_s))}{W_{ac}(kT_s)}\,, \tag{3}$$

where $M_{\max}(\xi)$ defines the maximum achievable load W_{ac}/ξ as a function of the engine speed ξ, and α_i, $i = 1,2,3$, are coefficients that depend on the engine and that can be identified by regression on experimental data.

The control input u is the ratio of in-cylinder air flow W_{ac} and in-cylinder fuel flow W_{fc},

$$u(k) = \frac{W_{ac}(kT_s)}{W_{fc}(kT_s)}\,. \tag{4}$$

The bounds on u depend on the transient fuel dynamics

$$\dot{m}_p(t) = -\frac{m_p(t)}{\tau_p} + XW_{fi}(t) \,, \tag{5a}$$

$$W_{fc}(t) = \frac{m_p(t)}{\tau_p} + (1-X)W_{fi}(t) \,, \tag{5b}$$

where m_p [kg] is the mass of the fuel in the fuel puddle formed at the ports, $\tau_p > 0$ [s] is the time-constant of puddle fuel evaporation, $X \in (0,1)$ is a fraction of the injected fuel that replenishes the liquid fuel puddle. In (5), W_{fi} [kg/s] is the mass flow of injected fuel,

$$0 \le W_{fi}(t) \le W_{f_{MAX}} \,, \tag{6}$$

where $W_{f_{\mathrm{MAX}}}$ [kg/s] is the maximum flow that the injectors can provide. Thus, from (4) and (5b) the input at step k is constrained in

$$\frac{W_{ac}(kT_s)}{\frac{m_p(kT_s)}{\tau_p} + (1-X)W_{f_{MAX}}} \le u(k) \le \frac{W_{ac}(kT_s)}{m_p(kT_s)}\tau_p \,, \tag{7}$$

where $m_p(kT_s)$ is computed from (5a) formulated as

$$\dot{m}_p(t) = -\frac{1}{1-X}\frac{m_p(t)}{\tau_p} + \frac{X}{1-X}\frac{W_{ac}(t)}{u(t)} \,.$$

2.2 Oxygen Storage Dynamics

For control purposes, the dynamics of the oxygen stored in the catalyst may be modelled by a constrained integrator [5]. The normalized catalyst oxygen storage $0 \le O(t) \le 1$ in the three-way-catalyst (TWC) evolves depending on the AFR,

$$\dot{O}(t) = W_{ac}(t)K\left(1 - \frac{1}{\lambda(t)}\right) \,, \tag{8}$$

where K is a known parameter, which may depend on the catalyst temperature and change with catalyst aging. Let $\Theta_c = O/W_{ac}$ and assume that W_{ac} is measured and varies slowly with respect to the AFR dynamics, so that for prediction purposes can be considered constant. Then, $\dot{\Theta}_c(t) = \dot{O}(t)/W_{ac}(t)$, and from (8)

$$\dot{\Theta}_c(t) = K\left(1 - \frac{1}{\lambda(t)}\right), \quad 0 \le \Theta_c(t) \le \frac{1}{W_{ac}(t)} \,. \tag{9}$$

Since for spark ignited engines the AFR varies in a small interval around 1, we can linearize (9), and convert it to discrete-time

$$\Theta(k+1) = \Theta(k) + T_s K(\lambda(k) - 1) \,, \tag{10a}$$

$$0 \le \Theta(k) \le \frac{1}{W_{ac}(kT_s)} \,. \tag{10b}$$

The oxygen storage dynamics (10a) is affine in Θ and λ. The airflow W_{ac} is a measured disturbance that can be assumed constant, hence (10b) is a parameter-dependent linear constraint.

3 Model Predictive Control with Delay Compensation

The most critical factor in AFR control is the time-varying delay that affects the command input $\tau_\lambda(k)$. The numerical value of $\tau_\lambda(k)$ can vary up to a factor of 10 over engine operating conditions, hence the MPC approaches for systems with constant delay [3] are not suitable. In order to cope with such a delay, we propose an architecture composed of the cascade of a delay compensator and a model predictive controller, as shown in Fig. 1. The delay compensator is a predictor based on AFR dynamics (2) and on oxygen dynamics (8).

In order to account for unmeasured disturbances and modeling imperfection due to transient fuel dynamics, a disturbance model [8] is added to the system which provides integral action. Since in AFR control the disturbances mostly take place in the fuel mixture in the cylinder, an input additive disturbance model is used. We define the state vector $z = [\lambda \; w \; \Theta \,]$, where w is the state of the disturbance model, so that the augmented system dynamics are

$$z(k+1) = Az(k) + Bu(k - \tau_\lambda(k)) + \nu + B_d v(k) \tag{11a}$$

$$\psi(k) = Cz(k) + e(k)\,. \tag{11b}$$

where ν is the affine term in (10a), $v(k)$, $e(k)$ are Gaussian variables with zero means and covariances P_v, P_e, respectively,

$$A = \begin{bmatrix} \alpha & \beta & 0 \\ 0 & 1 & 0 \\ KT_s & 0 & 1 \end{bmatrix}, \; B = \begin{bmatrix} \beta \\ 0 \\ 0 \end{bmatrix}, \; B_d = \begin{bmatrix} 0 \\ 1 \\ 0 \end{bmatrix}, \; \nu = \begin{bmatrix} 0 \\ 0 \\ KT_S \end{bmatrix}\,.$$

and $\psi(k)$ is the current measurement, where $C = [1\ 0\ 0]$. In (11), the state of the stored oxygen is not observable. The estimation of the oxygen in the catalyst is a rather complex operation [5], which is beyond the scope of this paper. We assume a low rate estimate of the oxygen storage is available, and we update the oxygen state in open-loop during the interval between two of such estimates.

3.1 State Predictor

The delay compensator performs two operations: (i) estimate the system state, and in particular the disturbance state w, (ii) predict the state of model (11) $\tau_\lambda(k)$ steps ahead to compensate for the delay. The first operation is performed by means of a Kalman Filter based on (11). The prediction is then computed by performing forward iterations of the system dynamics starting from the updated state estimate. Due to the discrete-time nature of the approach used here, perfect delay compensation is

not possible when $\tau_\lambda(k)$ is not a multiple of the sampling period T_s. In the following we assume that $\tau_\lambda(k) = cT_s$ for some nonnegative integer c. In case $\tau_\lambda(k)$ is not a multiple of T_s, the compensation is done with respect to $\tilde{\tau}_\lambda(k) = cT_s$, where c is the largest integer such that $c \leq \tau_\lambda(k)/T_s$, i.e., $c = \lfloor \tau_\lambda(k)/T_s \rfloor$. The prediction algorithm can be formalized as described in Algorithm 2.

Algorithm 2. Delay compensation by state prediction.

At time step k:

1. from current engine operating conditions ($\xi(k)$,$W_{ac}(k)$) estimates, $\tau_\lambda(k)$ using (3);
2. from current measurement $\psi(k)$ and previous state estimate $z(k-1)$ updates the state estimate $z(k) = [\lambda(k)\ w(k)\ \Theta(k)]$;
3. fix $\tau_\lambda(h) = \tau_\lambda(k)$, $W_{ac}(h) = W_{ac}(k)$ for all $h \in [k, k+\tau_\lambda(k)]$. From $z(k)$ and stored input $\mathbf{u}_p(k) = (u(k-\tau_\lambda(k-\tau_\lambda(k))), \ldots, u(k-1))$ predict the value $z(k+\tau_\lambda)$;
4. feed $x(k) = z(k+\tau_\lambda(k))$ to the the controller as the initial state.

In the prediction step of Algorithm 2 the prediction of the oxygen storage is obtained by using the nonlinear dynamics (9) instead of the linearized one (10a). By assuming that the airflow W_{ac} varies slowly with respect to the AFR dynamics, we can consider W_{ac} constant along the prediction horizon. Also, the time delay $\tau_\lambda(k)$ is assumed constant in prediction, since there is no preview on the future engine operating conditions. The prediction algorithm adapts to the time-varying delay, $\tau_\lambda(k)$. When the delay is large, e.g., at idle speed, the prediction will go far ahead in the future. When the delay is small, e.g., at high engine speed and airflow, the prediction will go ahead in the future only for a short time period. Algorithm 2 needs that a buffer is maintained to keep track of the past inputs. The length of the buffer must be dimensioned for a worst-case estimate $\bar{\tau}_\lambda \geq \max_k\{\tau_\lambda(k)\}$ of the delay.

By defining the variable $x(k) = z(k+\tau_\lambda(k))$ and using the certainty equivalence principle to remove the unpredictable unmeasured disturbance v, the system dynamics (11) formulated as prediction model is

$$x(k+1) = Ax(k) + Bu(k) + \nu\ , \tag{12}$$

where the delay has been removed and the system matrices A, B, ν are the same as in (11).

3.2 Model Predictive Controller

The delay-free model (12) can be used in a model predictive control strategy. At time k, Algorithm 2 is used to compute $x(k) = z(k+\tau_d(k))$. The time-varying constraint bounds on the input and on Θ are computed depending on the current value of the fuel puddle estimate $m_p(kT_s)$ and on the airflow $W_{ac}(kT_s)$.

At time k the input bounds $u_{\min}(k)$, $u_{\max}(k)$ are

$$u_{\min}(k) = \frac{W_{ac}(kT_s)}{\frac{m_p(kT_s)}{\tau_p} + (1-X)W_{f_{MAX}}}, \quad u_{\max}(k) = \frac{W_{ac}(kT_s)}{m_p(kT_s)}\tau_p \ , \tag{13}$$

and the state bounds $x_{\min}(k)$, $x_{\max}(k)$ are

$$x_{\min}(k) = \begin{bmatrix} \lambda_{\min} \\ -\infty \\ 0 \end{bmatrix}, \ x_{\max}(k) = \begin{bmatrix} \lambda_{\max} \\ +\infty \\ \frac{1}{W_{ac}(kT_S)} \end{bmatrix} \ , \tag{14}$$

where $\lambda_{\min}$, $\lambda_{\max}$ defines the boundary of the AFR value for which the three-way-catalyst can efficiently operates, and which shall not be crossed, unless for a very short time period. In this paper we use $\lambda_{\min} = 0.95$, $\lambda_{\max} = 1.05$, that are tightened with respect to the real desired range of operation being $\lambda \in [0.9, 1.1]$, in order to account for modeling imperfection and disturbances.

The MPC finite-time optimal control problem is

$$\min_{\mathbf{u}(k),\varepsilon} \quad \rho\varepsilon^2 + \tag{15a}$$

$$\sum_{i=0}^{N-1} (x(i|k) - \bar{x}(k))' Q (x(i|k) - \bar{x}(k)) + R\Delta u(i|k)^2$$

$$\text{s.t.} \quad x(i+1|k) = Ax(i|k) + Bu(i|k) + v \tag{15b}$$

$$x_{\min}(k) - \varepsilon \mathbf{1} \le x(i|k) \le x_{\min}(k) + \varepsilon \mathbf{1}, \ \ {\scriptstyle i=1,\ldots,N_c} \tag{15c}$$

$$u_{\min}(k) \le u(i|k) \le u_{\min}(k), \ \ {\scriptstyle i=0,\ldots,N} \tag{15d}$$

$$u(i|k) = u(N_u - 1|k), \ \ {\scriptstyle i=N_u,\ldots,N-1} \tag{15e}$$

$$\Delta u(i|k) = u(i|k) - u(i-1|k) \tag{15f}$$

$$x(0|k) = z(k + \tau_d(k)) \tag{15g}$$

$$u(-1|k) = u(k-1) \ , \tag{15h}$$

where N is the prediction horizon, $N_u \le N$ is the control horizon, the number of free moves to select, $N_c \le N$ is the constraint horizon, the number of steps along which state constraints are enforced, $\mathbf{u}(k) = (u(0|k), \ldots, u(N-1|k))$ is the input sequence to be optimized, and $\mathbf{1}$ indicates a vector of appropriate dimension entirely composed of 1.

In (15g), the optimization problem is initialized with state $z(k + \tau_d(k)) = \begin{bmatrix} \lambda(k+\tau_d(k)) & w(k) & \frac{O(k+\tau_d(k))}{W_{ac}(k)} \end{bmatrix}$ computed by Algorithm 2, and (12) is used for prediction by (15b).

In (15a), the vector $\bar{x}(k)$ is the desired state setpoint which remains constant along the prediction horizon, as well as the state and input bounds (15c), (15d). The state constraint (15c) is "softened" by the additional optimization variable ε, so that it can be violated, at the price of a largely increased cost. This prevents infeasibility

due to external unknown disturbances, and still enforces the desired range for AFR whenever possible.

We choose the weight R on input increments positive, and the weight matrix Q with the following structure $Q = \begin{bmatrix} q_1 & 0 & 0 \\ 0 & 0 & 0 \\ 0 & 0 & q_3 \end{bmatrix}$, where $q_1 \geq 0$ is the weight for AFR tracking and $q_3 \geq 0$ is the weight for oxygen storage tracking. The constraint violation weight $\rho \geq 0$ is chosen much larger than q_1, q_3, R. In (15) an incremental formulation of input cost is used, where the input variation $\Delta u(i|k)$ is weighted, which is more suitable for reference tracking.

The overall model predictive control algorithm with delay compensation is summarized in Algorithm 3.

Algorithm 3. Model predictive control with delay compensation for AFR and oxygen storage control.

At time step k:

1. execute Algorithm 2 from state $z(k-1)$, operating conditions $(\xi(k), W_{ac}(k))$, AFR measurement $\psi(k)$, and input buffer $\mathbf{u}_p(k)$ $\lambda(k)$ to obtain $z(k+\tau_\lambda(k))$;
2. set $x(k) = z(k+\tau_\lambda(k))$, solve optimal control problem (15a), and obtain the optimal input profile $\mathbf{u}^*(k) = (u^*(0|k), \ldots, u^*(N-1|k))$;
3. set the input $u(k) = u^*(0|k)$ and update $\mathbf{u}_p(k)$ by $u(k)$.

4 Simulation Results

In this section we discuss simulation results obtained from a detailed nonlinear model of AFR and oxygen dynamics in closed-loop with the MPC architecture of Sect. 3.2.

The controller objective is to track the references on the AFR and on the oxygen storage. In contrast with more classical approaches based on inner-outer loop control strategies, here we keep the reference of the AFR constantly to the stoichiometric ratio ($\lambda = 1$). The reference of the oxygen is slightly modulated around the middle point, since it is recognized that keeping the catalyst active improves the durability of the TWC. By this reference choice we investigate the capability of MPC in negotiating the different control objectives imposed by AFR and oxygen storage, using a single control input.

For the controller used in the simulations, in (15a) we have set $q_1 = 0.5$, $q_3 = 10^4$, $\rho = 10^7$, $N = 10$, $N_u = 2$, $N_c = 10$. A 10% error on W_{ac} is added, and an estimate of the stored oxygen is available at 0.1Hz, while the stored oxygen state is updated open-loop within two of such estimates. The reference for the AFR is $\lambda = 1$ while the oxygen reference is a square wave between 40% and 60% of its maximum value. We present two simulation scenarios. The first scenario is a demonstration of the controller behavior when the engine speed and airflow vary, in an acceleration and a deceleration. In the second scenario we test the controller with real airflow and engine speed profiles, obtained during the execution of an EPA driving cycle on a

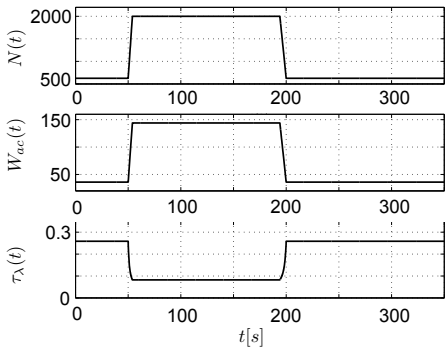

Fig. 2 Scenario 1, acceleration and deceleration. Engine speed, airflow and (estimated) time-delay profiles.

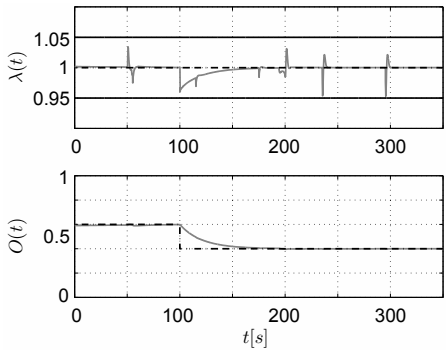

Fig. 3 Scenario 1, acceleration and deceleration. AFR and oxygen storage dynamics.

real vehicle. The first scenario involves acceleration and deceleration. The AFR is affected by an intermittent unmeasured additive input disturbance that models the purge of the fuel canister. When such purge happens an unknown amount of fuel is added to the one commanded by the controller. The engine speed is accelerated from idle speed (625 rpm) to 2000 rpm in 4s, then kept constant, and finally decelerated again to idle speed in 6s. At the same time, the airflow is increased from $W_{ac} =$ 36kg/hr to $W_{ac} = 144$kg/hr, then reduced again to $W_{ac} = 36$kg/hr. The profiles of W_{ac}, ξ, and τ_λ along this scenario are shown in Fig. 2. The results for the first scenario are shown in Fig. 3. The controller behaves correctly despite the variability in the time-delay due to different engine speed and airflow. Note that the effect of the fuel purge disturbance at high speed and high airflow is reduced due to the shorter time delay and because the fuel added by the purge is small compared to the commanded injection.

In the second scenario we simulate the controller action with respect to a real experimental airflow and engine speed profile obtained from a vehicle running the EPA drive cycle. In Fig. 4 the operating conditions, airflow and engine speed, and the

(estimated) time delay for $t \in [150, 350]$, are shown. In this segment of the profile, which includes acceleration from stationary conditions, cruising at about 60 miles per hour, and deceleration to stationary conditions again, the maximum variation of the time delay is of about a factor 10. As regards the oxygen storage, in this test we assume to have available measurements only when the oxygen level is very low ($O < 0.35$) or very high ($O > 0.75$), simulating the behavior of a heated exhaust gas oxygen sensor (HEGO) placed downstream of the TWC (see Fig. 1).

Despite the large variability in the time delay and the variations in the operating conditions, the controller is able to maintain the AFR in the desired operating range for most of the time, and the situations in which $\lambda \notin [0.9, 1.1]$ are extremely infrequent, as shown in Fig. 5. At the same time, the oxygen stored in the catalyst is maintained close to its desired value. The tracking error, acceptable for this type

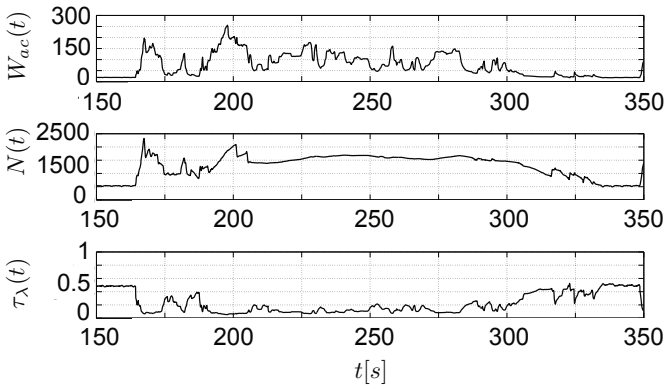

Fig. 4 Scenario 2, EPA test profile from real vehicle. Engine speed, airflow and (estimated) time-delay profiles.

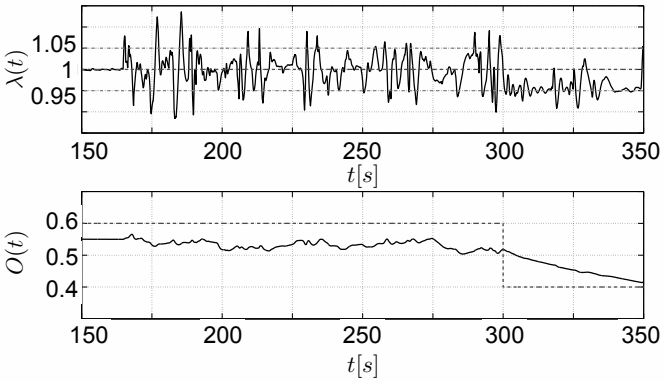

Fig. 5 Scenario 2, EPA test profile from real vehicle. AFR and oxygen storage dynamics.

of test, is mainly due to the fact that during this part of the simulation there is no available feedback from the HEGO for the stored oxygen, since $O \in [0.35, 0.75]$.

5 Conclusions

We have proposed a control architecture for negotiating the control of air-to-fuel ratio and oxygen storage in spark ignited engines. The control architecture is based on a delay-free model predictive controller, that enforces constraints on the actuators and on the operating range of the variables, and a delay compensation strategy based on a state predictor, that counteracts the time-varying delay that affects the system. Simulations in closed-loop with a detailed nonlinear model have been shown.

References

1. Beltrami, C., Chamaillard, Y., Millerioux, G., Higelin, P., Bloch, G.: AFR control in SI engine with neural prediction of cylinder air mass. In: Proc. American Contr. Conf., Denver, CO (2003)
2. Bemporad, A., Morari, M., Dua, V., Pistikopoulos, E.N.: The explicit linear quadratic regulator for constrained systems. Automatica 38(1), 3–20 (2002)
3. Di Cairano, S., Yanakiev, D., Bemporad, A., Kolmanovsky, I.V., Hrovat, D.: An MPC design flow for automotive control and applications to idle speed regulation. In: Proc. 47th IEEE Conf. on Decision and Control, Cancun, Mexico, pp. 5686–5691 (2008)
4. Fiengo, G., Cook, J., Grizzle, J.: Fore-aft oxygen storage control. In: Proc. American Contr. Conf., Anchorage, AK, pp. 1401–1406 (2002)
5. Guzzella, L., Onder, C.H.: Introduction to modeling and control of internal combustion engine systems. Springer, Heidelberg (2004)
6. Muske, K., Peyton-Jones, J., Franceschi, E.: Adaptive Analytical Model-Based Control for SI Engine Air–Fuel Ratio. IEEE Trans. Contr. Systems Technology 16(4), 763–768 (2008)
7. Ohata, A., Ohashi, M., Nasu, M., Inoue, T.: Model based air fuel ratio control for reducing exhaust gas emissions. In: Proc. SAE World Congress, Detroit, MI, page Paper 950075 (1995)
8. Pannocchia, G., Rawlings, J.B.: Disturbance models for offset-free model-predictive control. AIChE Journal 49(2), 426–437 (2003)
9. Powell, J., Fekete, N., Chang, C.: Observer-based air fuel ratio control. IEEE Control Systems Magazine 18(5), 72–83 (1998)